

**KERNFORSCHUNGSZENTRUM**

**KARLSRUHE**

Oktober 1967

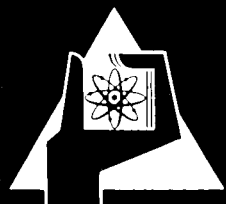
KFK 631  
SM 101/17  
EUR 3675 e

Institut für Neutronenphysik und Reaktortechnik

Energy and Temperature Dependent Capture Measurements  
below 30 keV Supporting Doppler Effect Calculations

H. Seufert, D. Stegemann

**LIBRARY**



Als Manuskript vervielfältigt

Für diesen Bericht behalten wir uns alle Rechte vor

Gesellschaft für Kernforschung m.b.H.

Karlsruhe

KERNFORSCHUNGSZENTRUM KARLSRUHE

Oktober 1967

KFK 631  
SM 101/17  
EUR 3675 e

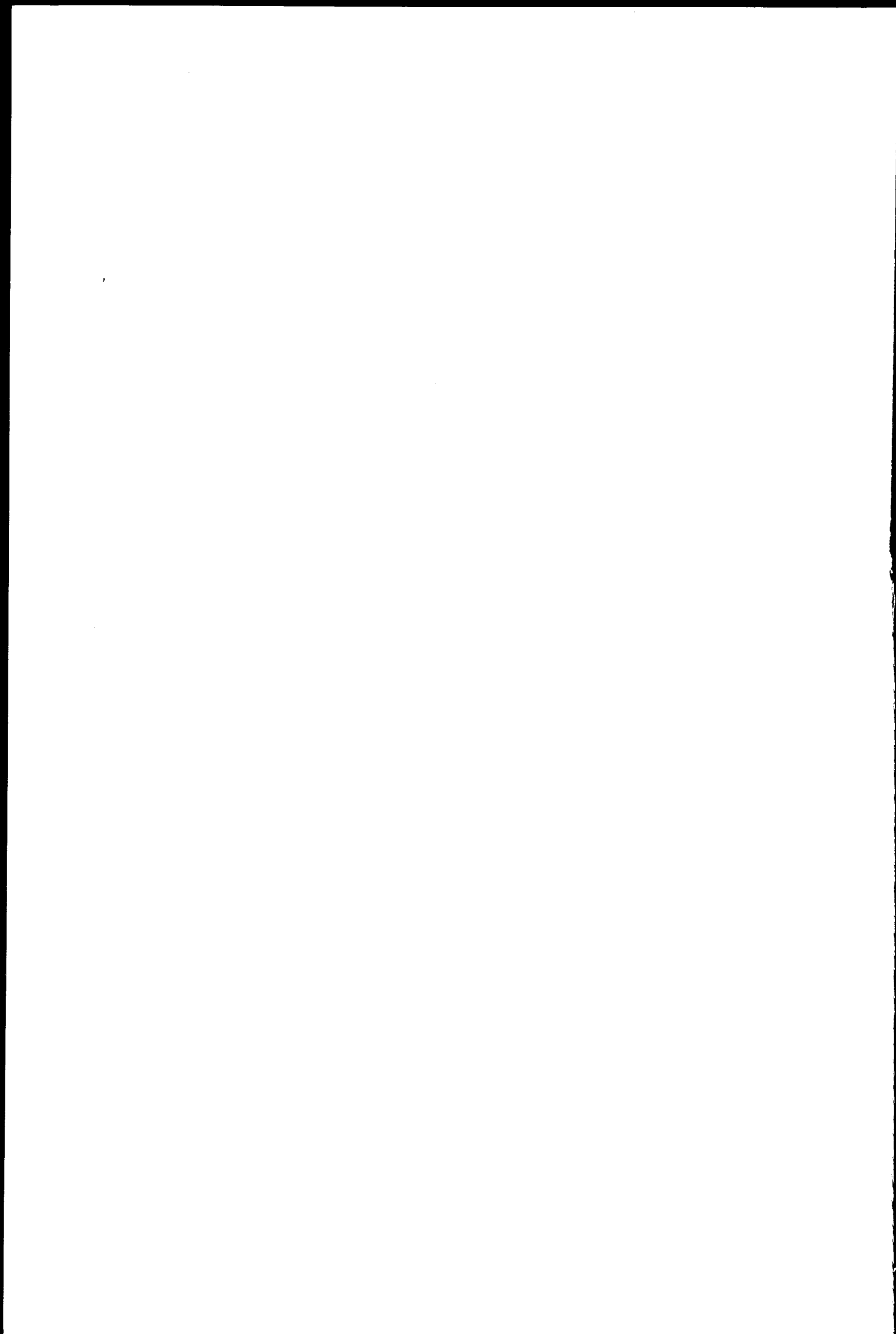
Institut für Neutronenphysik und Reaktortechnik

ENERGY AND TEMPERATURE DEPENDENT CAPTURE MEASUREMENTS  
BELOW 30 keV SUPPORTING DOPPLER EFFECT CALCULATIONS <sup>+</sup>

H. Seufert and D. Stegemann

<sup>+</sup> Work performed within the association in the field of  
fast reactors between the European Atomic Energy Community  
and Gesellschaft für Kernforschung m.b.H., Karlsruhe.

Gesellschaft für Kernforschung m.b.H., Karlsruhe



INTERNATIONAL ATOMIC ENERGY AGENCY

SYMPOSIUM ON FAST REACTOR PHYSICS AND  
RELATED SAFETY PROBLEMS

October 30 - November 3, 1967

Kernforschungszentrum Karlsruhe, Germany

SM 101/17

ENERGY AND TEMPERATURE DEPENDENT CAPTURE MEASUREMENTS  
BELOW 30 keV SUPPORTING DOPPLER EFFECT CALCULATIONS +

H. Seufert and D. Stegemann  
(presented by H. Seufert)

ABSTRACT

Energy and temperature dependent capture measurements below 30 keV neutron energy have been performed in natural uranium, tungsten, and tantalum using the slowing down time spectrometer technique. The experimental setup used for the experiments consists of a lead block of 1.3 m side length containing two experimental channels of  $10 \times 10 \text{ cm}^2$  cross-section. Into the first channel the target of a 14 MeV neutron generator is introduced, whereas the second channel is used for insertion of the heated samples. Pulses of 14 MeV-neutrons, having a pulse width of about  $1/\mu\text{sec}$  are used. The neutron energy is degraded first by inelastic collisions; afterwards only elastic collisions take place so that a specific relationship holds between mean neutron energy in the lead pile and the time after occurrence of the neutron pulse. Due to this time-energy relation a time analysis procedure for the detector counts is applied.

Because the energy range below 30 keV neutron energy is most interesting for Doppler-effect investigations the slowing down time spectrometer is used to measure the capture ratios of hot-to-cold samples of natural uranium, tungsten, and tantalum. Thin samples were heated to different temperatures for this purpose, and the capture  $\gamma$ -rays were detected by proportional counters. Because hot-to-cold capture ratios are measured the knowledge of the neutron flux is not necessary; therefore, a direct comparison of calculated and measured temperature dependent cross-sections is possible. A theoretical analysis of the experimental data for uranium is given.

+ Work performed within the association in the field of fast reactors between the European Atomic Energy Community and Gesellschaft für Kernforschung mbH., Karlsruhe.

## 1. INTRODUCTION

The idea to measure temperature and energy dependent reaction rates was thought to be necessary in order to support the analysis of integral Doppler experiments performed in fast critical assemblies. This support concerns only the neutron and nuclear physics aspects of Doppler-effect analysis separately from the additional reactor physics complications in order to reduce the problems for a detailed comparison of experiment with theory. Besides the Doppler-effect of fissile and fertile reactor materials the study of high temperature metals like tungsten and tantalum is also of interest in advanced high temperature reactors.

The aim of this experiment was the measurement of energy dependent reaction rates below 30 keV at different sample temperatures. For this purpose the neutron slowing down time spectrometer  $\overline{1,2}$  was used, which operates as follows: Fast monoenergetic neutron bursts of short duration are slowed down in a material of high mass number in which they maintain a relatively narrow energy distribution. Therefore, a relation holds between slowing down time and average neutron energy. The moderator, a lead cube, contains an experimental channel into which the sample under investigation is positioned. Neutron captures in the sample result in spontaneous  $\gamma$ -rays from the decaying nuclei. These capture  $\gamma$ 's are measured time-dependent by proportional counters. By this procedure hot-to-cold reaction rate ratios between 0.2 and 30 keV were measured in similar time-dependent neutron spectra. Because of this the neutron flux cancels almost completely in the hot-to-cold ratio formed, which is an important advantage of this experiment. Apart from this the resonance energy region of interest for Doppler experiments coincides with the energy range covered by the slowing down time spectrometer, so obtaining an optimum energy dependent signal of the Doppler-effect at different temperatures.

This type of experiment is well suited to check theoretical analysis regarding to uncertainties in nuclear data and correct calculation of temperature dependent cross sections in the statistical region of resonances including resonance interference and overlap effects of different isotopes present in one mixture. The results from these experiments are a helpful tool for the analysis of energy integrated foil activation measurements or other Doppler experiments in fast reactors.

## 2. EXPERIMENTS AND RESULTS

### 2.1 Description of experimental setup

A sketch of the experimental setup is shown in Fig.1. The main components are the neutron generator and the lead cube of 1.3 m side length. Highly purified lead (99.99 %) was used for the slowing down time spectrometer. Two channels of  $10 \times 10 \text{ cm}^2$  cross section were cut out of the lead cube, one for the target, one for the sample under investigation. The lead cube was surrounded by a 1 mm thick Cd-sheet to prevent reentrance of slow neutrons. Short neutron bursts were generated by the reaction  $T(d,n)\alpha$  with a pulsed Cockroft-Walton type accelerator. The titanium-tritium target placed in the center of the lead cube was bombarded by the deuterons accelerated up to 150 keV. The ions from a Penning type source were accelerated in dc operation and the ion pulses of 0.4 to 1.5  $\mu\text{s}$  duration were formed by deflection plates as indicated in Fig.1. The pulse repetition rate was 2 k cps for nearly all experiments.

### 2.2 Detectors, furnaces, and electronics

Three experimental runs, two at different sample temperatures and one background measurement, are necessary to evaluate the hot-to-cold capture ratio. To make intercomparison between the three runs the neutron source strength had been monitored by a  $\text{BF}_3$  proportional counter shielded with Cd against slow neutrons. Its position is indicated in Fig.1.

Fig.2 shows the cross sections of the two different furnaces used in these experiments. In assembly A the sample is surrounded by the detector in contrast to assembly B. The detectors were proportional counters of 30 cm sensitive length and 10 mm diameter at 1 mm wall thickness. They were filled with argon at a pressure of 760 mm Hg. Two assemblies A and B were constructed because different aspects had to be taken into account. One aspect is the optimum detector efficiency obtained by maximum solid angle in order to have reasonable counting times. Another aspect concerns a maximum signal-to-background ratio, which is of utmost importance if the sample cross section is low. Assembly A is best suited for large cross section samples because it has approximately  $4\pi$  geometry. Assembly B, on the other hand, offers maximum signal-to-background ratio. The disadvantage, however,

is the reduced detector efficiency. For the geometry shown in Fig.2, A and B, the background is reduced by a factor of 10 from assembly A to B. The corresponding efficiency (solid angle) is only reduced by a factor of around 4 from A to B. This has been found from calculations. Therefore, assembly B had to be used to measure capture in  $^{238}\text{U}$ .

For the furnace constructions in Fig.2 some additional informations are given: All furnace material including the electrical feed throughs and proportional counter tubes were fabricated from AlMg3 an alloy (97% Al, 3% Mg) having an extremely low capture cross section. The volume between the inner and outer furnace wall was evacuated up to  $10^{-4}$  Torr by a diffusion pump to avoid heat convection. The sample is heated by 1 mm thermocoax wires. The heating power necessary to achieve a sample temperature of  $700^{\circ}\text{K}$  was 12 watts for assembly A and 70 watts for assembly B. Temperature was measured by NiCr-Ni thermocouples. All inner surfaces were polished in order to have high reflection of heat radiation.

The electronic circuitry is shown in Fig.3. The monitor channel is conventional electronics. The special kind of signal channel shall be explained in more detail. Actually two detectors feed one linear channel with pulses. The signals of the five channels are mixed and afterwards time-analyzed. These five channels were found to be necessary because during and shortly after the neutron bursts high  $\gamma$ -flux impinges onto the detectors. Using five channels instead of one results in a considerable reduction of pulse pile-up. Conventional non-overload amplifiers have-for these high amplitude input pulses-long recovery times and base line shifts. The mixer of the five channel circuitry delivers fast output signals of 100 ns pulse width and had a time resolution of the same order. The pulses were finally analyzed by a fast shift register <sup>1)</sup>  $\underline{\underline{37}}$ . The maximum counting speed together with the multiscaler storage system was  $5 \cdot 10^6$  pulses per second in every channel. Conventional time analyzers could not be used for these measurements due to deadtimes of the order of  $10/\mu\text{s}$ . So they cannot handle the counting rates of about  $2 \cdot 10^5$  pulses per second during and shortly after the neutron bursts. In this setup the limiting factors concerning deadtime were the amplifiers and discriminators used in the counting channels having about 2 to  $3/\mu\text{s}$  deadtime so, in this respect, the setup was not optimum.

<sup>1)</sup> Manufactured by BORER and Co., Solothurn-Switzerland.



Besides a demand for extremely short deadtimes the total drift in countrate should be better than 0.5 % per 10 hours, for measuring times of several hours are possible only in this way. Long measuring times, however, are necessary to achieve good statistics. The main instabilities result from drifts of discriminator levels and less from gain variations of amplifiers. In Fig.4 the  $\gamma$  pulse height spectrum of a proportional counter is shown. The discriminator level has been set according to the indication in Fig.4. The necessary long time behavior was even better than 0.5 % in our arrangement.

### 2.3 Energy calibration of slowing down time spectrometer

The relation between average neutron energy and slowing down time for an elastic scattering medium is given by:

$$\bar{E}(t) = \frac{m_N A^2 \lambda_s^2}{2} \frac{1}{\left(t + \frac{A \lambda_s}{v_0}\right)^2} \quad (2.1)$$

or

$$t = \sqrt{\frac{C}{E}} - t_0 \quad (2.2)$$

with

$$C = \frac{m_N A^2 \lambda_s^2}{2}$$

$$t_0 = \frac{A \lambda_s}{v_0}$$

The symbols are explained in the nomenclature given at the end of this paper. To calibrate the spectrometer in the energy range under investigation two different materials with resonances of known energies were measured. A plot of slowing down time versus  $1/\sqrt{E}$ , shown in Fig.5, is best suited to compare the constant C with earlier calibrations [2]. The result is  $C = 185 \text{ keV} \mu\text{s}^2$  compared to  $179 \text{ keV} \mu\text{s}^2$  of [2]. The resonance energies were taken from BNL-325.

To avoid the influence of higher harmonics of the spatial neutron distribution on energy calibration the  $\gamma$ -detectors were positioned at zero crossing of the third harmonic as indicated in Fig.1.

## 2.4 Resolution of slowing down time spectrometer

The energy resolution is determined on the one hand by the slowing down phenomena, on the other hand by uncertainties in the time measurement and the extended neutron pulse width. The following three slowing down phases are mainly responsible for the energy resolution of the spectrometer:

1. Inelastic scattering above 0.5 MeV.
2. Asymptotic energy distribution resulting from the statistics of scattering below the first excited level.
3. Thermal motion of lead atoms at eV-energies.

The calculated energy resolution as function of slowing down time is plotted in Fig.6 taking into account all effects mentioned above (neutron pulse width 1.5  $\mu$ s).

The resolution of the spectrometer is appropriate for measuring the energy dependent resonance integral in the statistical energy region from 0.2 to 30 keV. As is more fully explained in section 3 the following condition must hold:

$$\overline{\Gamma}_n^s, \Gamma_\gamma \ll \overline{D}^s \ll \Delta E \ll E \quad (2.3)$$

It can be seen from Fig.6 that (2.3) is satisfied.

## 2.5 Deadtime effects and test measurements

The high counting rates during and shortly after the neutron bursts (the reasons for this effect are summarized in  $\overline{[2]}$ ) could not be registered without counting losses due to the deadtime limit explained in 2.2. To investigate the influence of deadtime effects on the hot-to-cold  $\gamma$ -ray ratio the following experiment was carried out. The basic idea of this experiment is to simulate the increased counting rate from the Doppler-effect by higher neutron intensity. The procedure is explained by the following formula (2.4):

$$\frac{S_{I_1}(t) - B_{I_1}(t)}{S_{I_2}(t) - B_{I_2}(t)} \quad (2.4)$$

with

- S - signal plus background at  $I_1$  and t
- B - background at  $I_1$  and t
- $I_i$  - neutron intensity i
- t - slowing down time.

This ratio is very similar to the hot-to-cold  $\gamma$ -ray ratio of a real experiment defined by:

$$R = \frac{H(t) - B(t)}{C(t) - B(t)} \quad (2.5)$$

with H - signal plus background of hot sample at t  
C - signal plus background of cold sample at t  
B - background at t .

The only difference between (2.4) and (2.5) is that the background depends on neutron intensity in (2.4). However, (2.4) and (2.5) are almost equal in our case and a measurement approximates the deadtime effect closely. In Fig.7 the result of a deadtime experiment is shown in which tantalum has been measured at two neutron intensities differing by 9.5 %. Up to the fifth channel the deadtime loss is large and affects the accuracy of hot-to-cold  $\gamma$ -ray ratios appreciably. Consequently we reduced the deadtime effects in the first five channels by running the neutron generator at reduced power, which means 110 kV accelerating voltage and 2 ma target ion current for nearly all measurements.

Another effect which was investigated concerns the  $\gamma$ -shielding of the detectors by the samples to be measured. Very thick samples absorb  $\gamma$ -rays from the lead and, therefore, change background. Fig.8 shows the result of such a shielding experiment where a 0.2 mm thick lead foil was used replacing the sample. The thickness of this foil was sufficient to simulate the  $\gamma$ -absorption effect of the samples investigated. The measurement shows that the absorption effect on background can be neglected.

Finally, it was necessary to measure the ratio of heated-to-cold empty furnace to make sure that the heating itself does not contribute to the hot-to-cold ratio of a sample measurement. For a temperature change of 400°C the result is plotted in Fig.9. This includes the influence of furnace dislocations by heating. This, too, is of no concern to the results.

## 2.6 Measurements with $^{238}\text{U}$

For  $^{238}\text{U}$  the ratio of the  $\gamma$ -counting rates obtained with the heated sample to the  $\gamma$ -counting rate with the sample at room temperature, after subtraction of background (hot-to-cold  $\gamma$ -ray ratio), is shown as function of average energy or slowing down time in Fig.10 and 11, respectively.

The experimental conditions - also used for the theoretical calculations according to paragraph 3 - are given in TABLE I. The experimental results are shown by crosspoints and the theoretical calculation is presented by the dashed curve. The error margins given are based only on statistics at 68% confidence level. They are evaluated from the formula

$$\frac{\Delta R}{R} = \frac{1}{(H-B)(C-B)} \sqrt{(C-B)^2 H + (H-C)^2 B + (H-B)^2 C} \quad (2.6)$$

which is derived from (2.5) with the error propagation law. In order to reduce the error margins of the experiment a faster electronic circuitry for the linear channels is necessary and now under construction for future experiments. A statistical error in R-1 of about 5 to 10% is aimed for. In spite of the limited accuracy the experimental data seem to indicate the possibility to interpret the capture rate increase (see paragraph 3) by statistical theory down to several hundred eV.

$^{238}\text{U}$  is of special interest to Doppler investigations in fast reactors and justifies further efforts to improve accuracy. In this conjunction, however, a number of difficulties have to be mentioned which are particular to  $^{238}\text{U}$ . The main difficulty results from the low signal-to-background ratio, which means that  $\gamma$ 's from lead contribute to the counting rate almost as much as the capture  $\gamma$ 's of the sample itself. The disadvantage from this effect follows directly from the first term of eq.(2.6). In order to minimize the background the  $\gamma$ -rays resulting from the decays of  $^{238}\text{U}$  and impurities had been nearly eliminated by shielding the detectors with 300 microns lead as indicated in Fig.2B. Another difficulty arises from the oxidization of uranium metal at elevated temperatures. To avoid this we have put the foil between two closely spaced aluminium tubes welded at the ends. Because of the small volume left almost no oxidization took place.

### 2.7 Measurements with tantalum and tungsten

For natural tantalum and tungsten measured hot-to-cold  $\gamma$ -ray ratios versus energy are shown in Fig.12 and Fig.13. The experimental conditions are shown in TABLE II. Furnace type A has been used for these experiments. The solid lines are fits to the experimental data. Theoretical calculations for both materials have not been done so far. Fig.12 is the average of three runs under same conditions which had been performed to check reproducibility. The error margins for tantalum are much smaller than for  $^{238}\text{U}$  due to a better signal-to-background ratio of about 3. The accuracy obtained for tantalum shows the capability of this method for Doppler-effect investigations if the conditions are optimized.

### 3. CALCULATION OF CAPTURE RESONANCE INTEGRALS AT DIFFERENT ENERGIES

#### 3.1 The analytic model of the heterogeneous resonance integral

We have the following experimental arrangement. The absorber, an isotope of high mass number, is surrounded totally by the slowing down material lead. Because the energy width of an absorber resonance is small against the energy loss of neutrons by elastic collisions in both the absorber and surrounding moderator, heterogeneous resonance integral theory in narrow resonance approximation can be applied for this situation. We follow the derivation of DRESNER [4] for the heterogeneous resonance integral. It is defined in our case as the energy integrated absorption cross section which, when multiplied by the flux  $\phi$  that would exist in the absence of the resonance, gives the true absorption rate:

$$N I \phi V = \int_{\Delta E} N \sigma_a \phi V dE \quad (3.1)$$

with

$$I = \frac{1}{\Delta E} \int \frac{\Sigma_p \sigma_a}{\Sigma_t} dE + \frac{1}{\Delta E} \int \frac{(\Sigma_t - \Sigma_p) \sigma_a}{\Sigma_t} P_o(\Sigma_t) dE \quad (3.2)$$

(3.2) can be rewritten with WIGNER's rational approximation for  $P_o(\Sigma_t)$

$$I = \frac{1}{\Delta E} \int \sigma_a(T) \frac{S + \Sigma_p}{S + \Sigma_t(T)} dE \quad (3.3)$$

with  $S = \frac{1}{1}$  .

This formula used for our experiments is identical to the selfabsorption term of the theoretical treatment of Doppler foil activation measurements as performed by A.B. REYNOLDS [5].

#### 3.2 Calculation of the $^{238}\text{U}$ -resonance integral from nuclear data

In this paragraph the way of calculating (3.3) is specified. The range of calculation has been limited to the statistical energy region because this mainly contributes to the Doppler-effect in fast reactors. In this paper we have restricted ourselves to capture processes in  $^{238}\text{U}$ , because also  $^{238}\text{U}$  foil activation experiments were carried out at the STARK-reactor [6]. Capture in monoisotopic nuclides like  $^{181}\text{Ta}$  are treated correspondingly.

For  $^{238}\text{U}$  the three resonance series are given below

l	0	1	1
j	1/2	1/2	3/2
s	1	2	3

The resonances are described in the multi-channel one level approximation by:

$$\sigma_t(x) = \sigma_{oc} \left( \frac{1}{1+x} \cos 2\delta_1 + \frac{x}{1+x} \sin 2\delta_1 \right) + \sigma_p \quad (3.4)$$

$$\sigma_a(x) = \sigma_{oa} \frac{1}{1+x} \quad (3.5)$$

with  $x = \frac{2}{\Gamma} (E - E_R)$

At low energies the asymmetric term in (3.4) disappears because of small  $\delta_1$  and will be neglected in the following treatment.

Conventional methods [4] have been used to calculate the temperature dependent Doppler-effect, i.e. the temperature dependent resonance integral (3.3). Using the abbreviations

$$N \sigma_p' = \Sigma_p' = \Sigma_p + S$$

$$N \sigma_t' = \Sigma_t' = \Sigma_t + S$$

we get

$$I = \sum_s \frac{\sigma_p' \Gamma_\gamma}{\Delta E \cos 2\delta_1^s} J(\theta^s, \beta^s) \quad (3.6)$$

with  $\theta^s = \frac{\Gamma^s}{\Delta}$

$$\beta^s = \frac{\sigma_p'}{\sigma_{oc}^s \cos 2\delta_1^s}$$

Because the nuclear resonances are very narrow the energy dependence of  $\theta^s$  and  $\beta^s$  are ignored over the range of integration. Besides this, it has to be summed over the different resonance series (index s).

In the statistical resonance region the resonance integral (3.6) has to be averaged over the Porter-Thomas statistical chi-squared  $\Gamma_n$  distribution of one degree of freedom. The radiative capture width  $\Gamma_\gamma$  is taken to be constant. We did this averaging according to a method described in [7].

Finally, the energy range of integration  $\Delta E$  must be chosen. So far we have assumed only one resonance in  $\Delta E$ . In reality we had  $n^s$  resonances in  $\Delta E$  due to the limited energy resolution of the neutron spectrometer.

With the aid of

$$\frac{\Delta E}{n^s} = \overline{D^s} \quad (3.7)$$

(3.6) can be rewritten:

$$I = \sum_s \frac{\sigma_p' \Gamma_\gamma}{\overline{D^s} \cos 2\delta_1^s} J(\theta^s, \beta^s) \quad (3.8)$$

The average energy dependent level spacing was calculated from the average level density.

### 3.3 A code for the calculation of the resonance integral

A code has been written for the IBM 7074 to calculate hot-to-cold foil activation ratios containing as an option hot-to-cold resonance integral ratios. This code computes the hot-to-cold ratios using the formulas and averaging methods mentioned in 3.1 and 3.2. No resonance overlap corrections have been applied. The basic nuclear data, which are incorporated into the code for  $^{238}\text{U}$ , are taken from J.J. SCHMIDT [8] and given in TABLE III.

The tabulated J-integral was used except for small  $\theta$  and  $\theta/\beta$  values for which DRESNER [4] has given a power series yielding an accurate solution. Computer running time for one ratio at one energy is 8 minutes.

## 4. DISCUSSION AND CONCLUSIONS

The investigations described have demonstrated the possibility to use the slowing down time spectrometer in the energy range from 0.2 to 30 keV to measure the Doppler-effect of heated samples. For these experiments the limited energy resolution of the spectrometer is advantageous because averaging over  $\Delta E$  is necessary to compare experiment with theory in the statistical energy region. The experiments described here have to be taken as a first step to look into the capabilities of the slowing down time spectrometer for this type of investigations. Although sufficiently small error margins have been obtained, for instance, for tantalum an improvement is

necessary for materials with low signal to background ratios, i.e.  $^{238}\text{U}$ . This improvement can certainly be reached by use of faster electronics decreasing deadtime effects. From the result of  $^{238}\text{U}$  obtained so far it can be concluded that an accuracy of the measured ratio of about 5 to 10% seems to be possible.

Further, it can be concluded from the experience gained so far that other interesting aspects of Doppler-effect can be investigated by this technique as there are: Overlap and interference effects of different resonance series and different nuclides, the low energy extension to which the statistical resonance theory holds and the saturation range of the Doppler-effect at high temperatures.

#### ACKNOWLEDGEMENTS

The authors acknowledge the recommendations of nuclear data by J.J. SCHMIDT. Further, we thank H. HELMKE for his help during the setup of the experiments.



## REFERENCES

- [1] BERGMAN, A.A. et al., A Neutron Spectrometer Based on Measuring the Slowing-Down Time of Neutrons in Lead, Proc. Geneva Conf. (1955) IV 135
- [2] MITZEL, F., PLENDL, H.S., Messungen von (n, $\gamma$ )-Wirkungsquerschnitten und Resonanzintegralen mit dem Bleispektrometer, Nukleonik 6 8 (1964) 371
- [3] EDELMANN, M. et al., Investigation of Prompt Neutron Kinetics in the Fast-Thermal Argonaut-Reactor STARK by Noise Analysis, KFK 522, Kernforschungszentrum Karlsruhe
- [4] DRESNER, L., Resonance Absorption in Nuclear Reactors, Pergamon Press, New York (1960)
- [5] REYNOLDS, A.B., Resonance Integral for the Doppler Measurement in Fast Reactors by the Foil-Activation Technique, Nucl. Sc. Eng. 22 (1965) 487
- [6] SEUFERT, H., to be published
- [7] FERZIGER, J.H. et al., Resonance Integral Calculations for Evaluation of Doppler Coefficients (The Rapture Code), USAEC Rep. GEAP 3923
- [8] SCHMIDT, J.J., Neutron Cross Sections for Fast Reactor Materials, Part I: Evaluation, KFK 120, Kernforschungszentrum Karlsruhe.

## NOMENCLATURE

A	- Atomic mass (mass units)
$\delta_1$	- Phase shift for neutrons with quantum number 1
$\overline{D^s}$	- Mean level spacing of serie s (eV)
$\Delta$	- Doppler width (eV)
E	- Energy (eV)
$\Delta E$	- Energy range (eV)
$\overline{E}$	- Mean energy (eV)
$E_R$	- Resonance energy (eV)
$\Gamma$	- Total width (eV)
$\Gamma_\gamma$	- $\gamma$ -width (eV)
$\overline{\Gamma_n^s}$	- Neutron width of serie s (eV)
I	- Effective resonance integral (barns)
J	- J-integral
j	- Spin quantum number of compound nucleus
$\overline{l}$	- Mean chord length (cm)
$\lambda_s$	- Scattering mean free path (cm)
l	- Angular momentum quantum number of compound nucleus
$m_N$	- Neutron mass (mass units)
N	- Density of sample material (cm <sup>-3</sup> )
$P_0$	- Escape probability
R	- Hot-to-cold $\gamma$ -ray ratio
s	- Number of resonance serie
$\sigma_a$	- Microscopic absorption cross section (barns)
$\sigma_p$	- Potential cross section (barns)
$\sigma_t$	- Total cross section (barns)
$\sigma_{oc}$	- Compound nucleus cross section at $E = E_R$ (barns)
$\sigma_{oa}$	- Absorption cross section at $E = E_R$ (barns)
$\Sigma_p$	- Macroscopic potential cross section (cm <sup>-1</sup> )
$\Sigma_t$	- Macroscopic total cross section (cm <sup>-1</sup> )
$\sum$	- Summation symbol
t	- Slowing down time ( $\mu$ s)
T	- Temperature ( $^{\circ}$ K)
V	- Volume (cm <sup>3</sup> )
$\emptyset$	- Flux in $\Delta E$ (cm <sup>-2</sup> s <sup>-1</sup> )
$\Phi$	- Flux per energy unit (cm <sup>-2</sup> s <sup>-1</sup> eV <sup>-1</sup> ).

Hot sample temperature ( $^{\circ}\text{K}$ )	750
Cold sample temperature ( $^{\circ}\text{K}$ )	300
Toil thickness (microns)	155
Toil length (cm)	25
Toil weight (g)	51.33
$\sigma_p$ (barns)	14

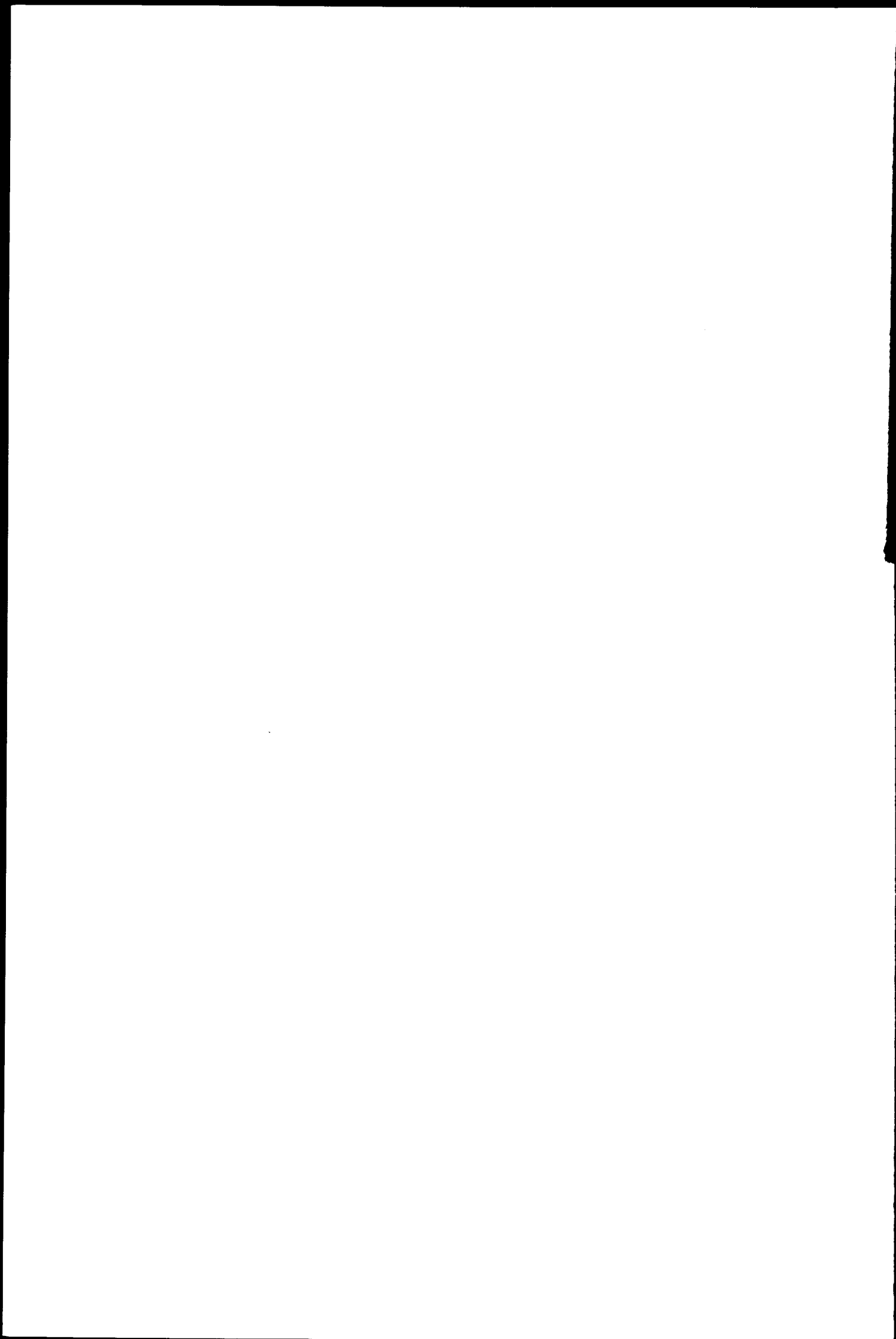
TABLE I Parameters for the  $^{238}\text{U}$ -measurement

	Tantalum	Tungsten
Hot sample temperature ( $^{\circ}\text{K}$ )	700	700
Cold sample temperature ( $^{\circ}\text{K}$ )	300	300
Foil thickness (microns)	150	350
Foil length (cm)	30	25
Foil weight (g)	35.19	68.75

TABLE II Parameters for the tantalum and tungsten measurements

s	1	2	3	
$E_B$		$4.76 \cdot 10^6$		eV
$\overline{D^0}$	20.8	20.8	11.4	eV
$\Gamma_{\gamma}$		24.8		meV
$\overline{\Gamma_n^0}$	1.87	5.2	2.85	meV
R		9.18		f

TABLE III Recommended Nuclear Data for  $^{238}\text{U}$



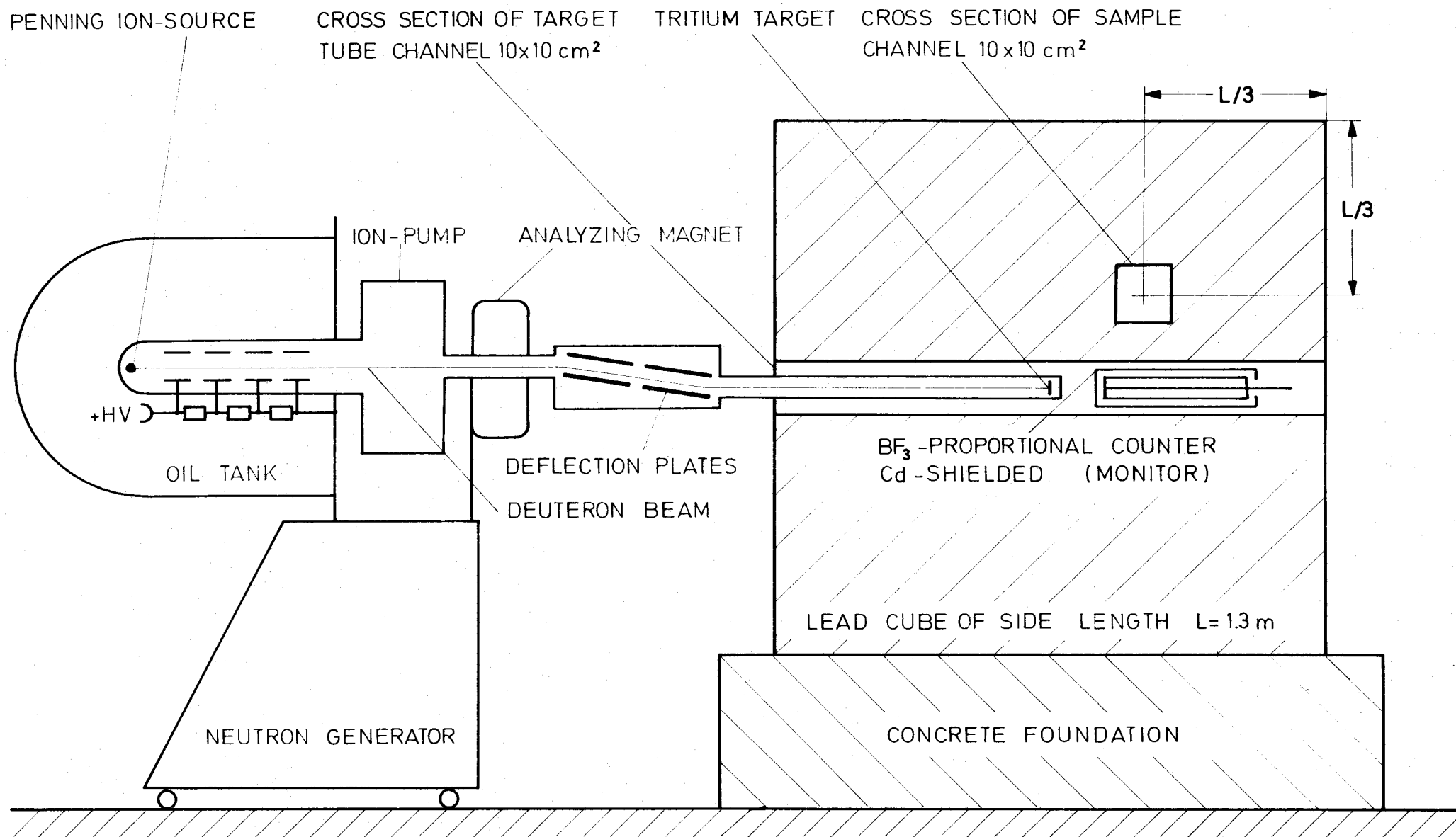


FIG.1 SETUP OF NEUTRON SLOWING DOWN TIME SPECTROMETER

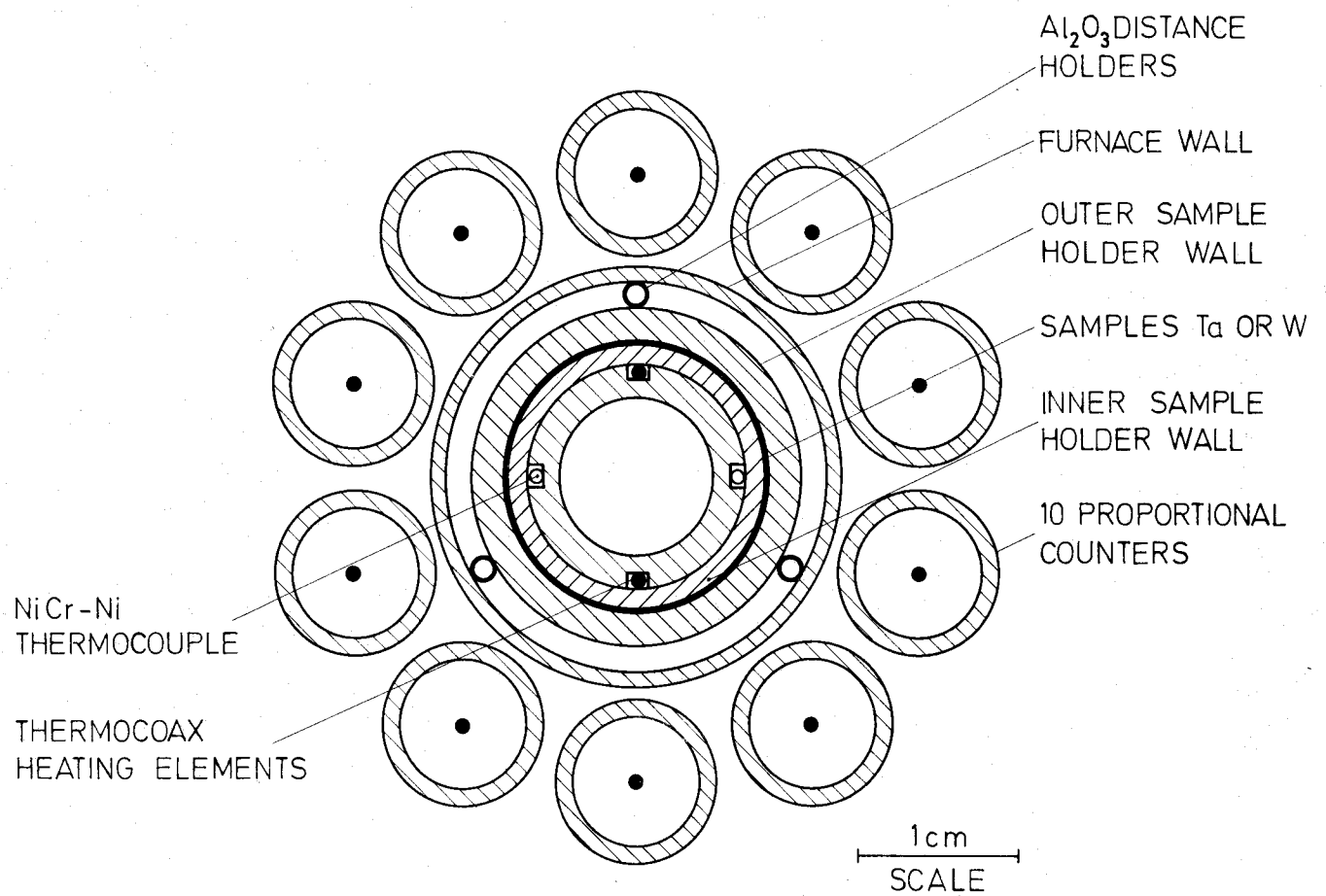


FIG.2A PROFILE OF FURNACE ASSEMBLY A

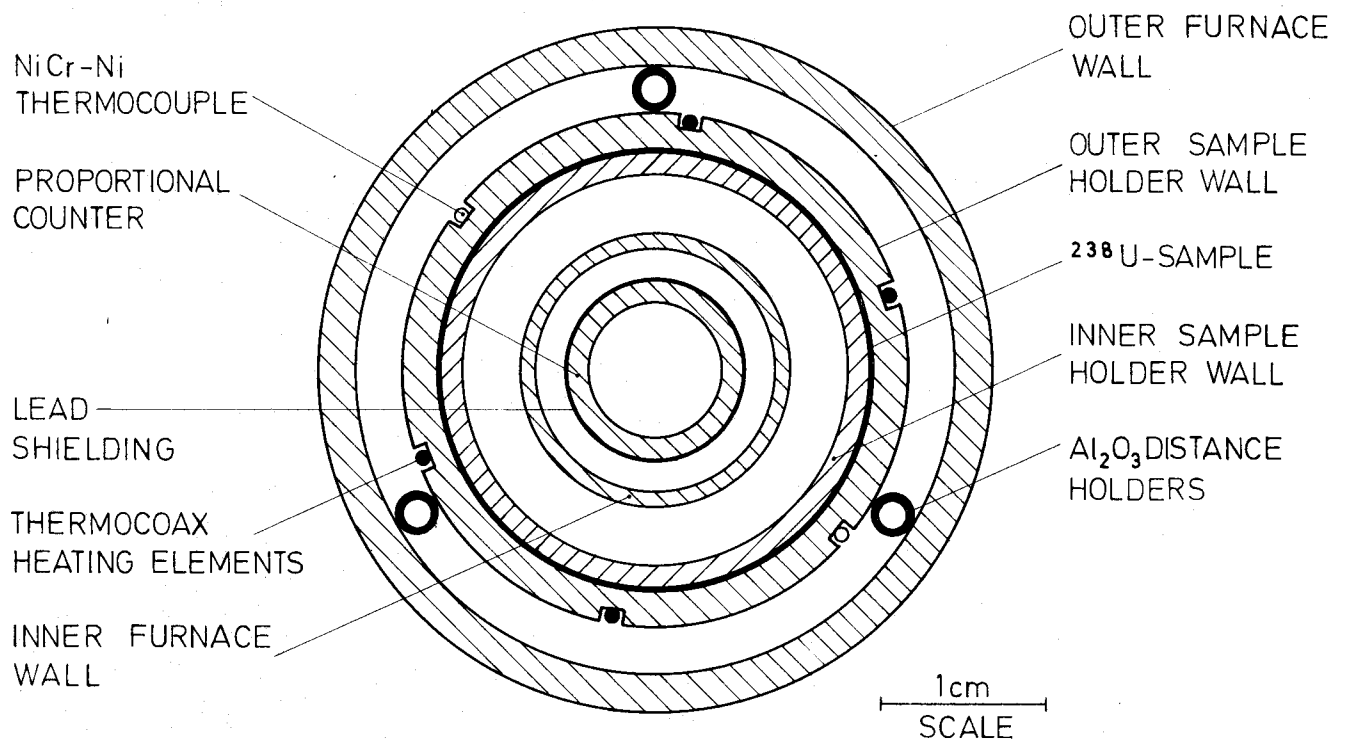


FIG.2B PROFILE OF FURNACE ASSEMBLY B

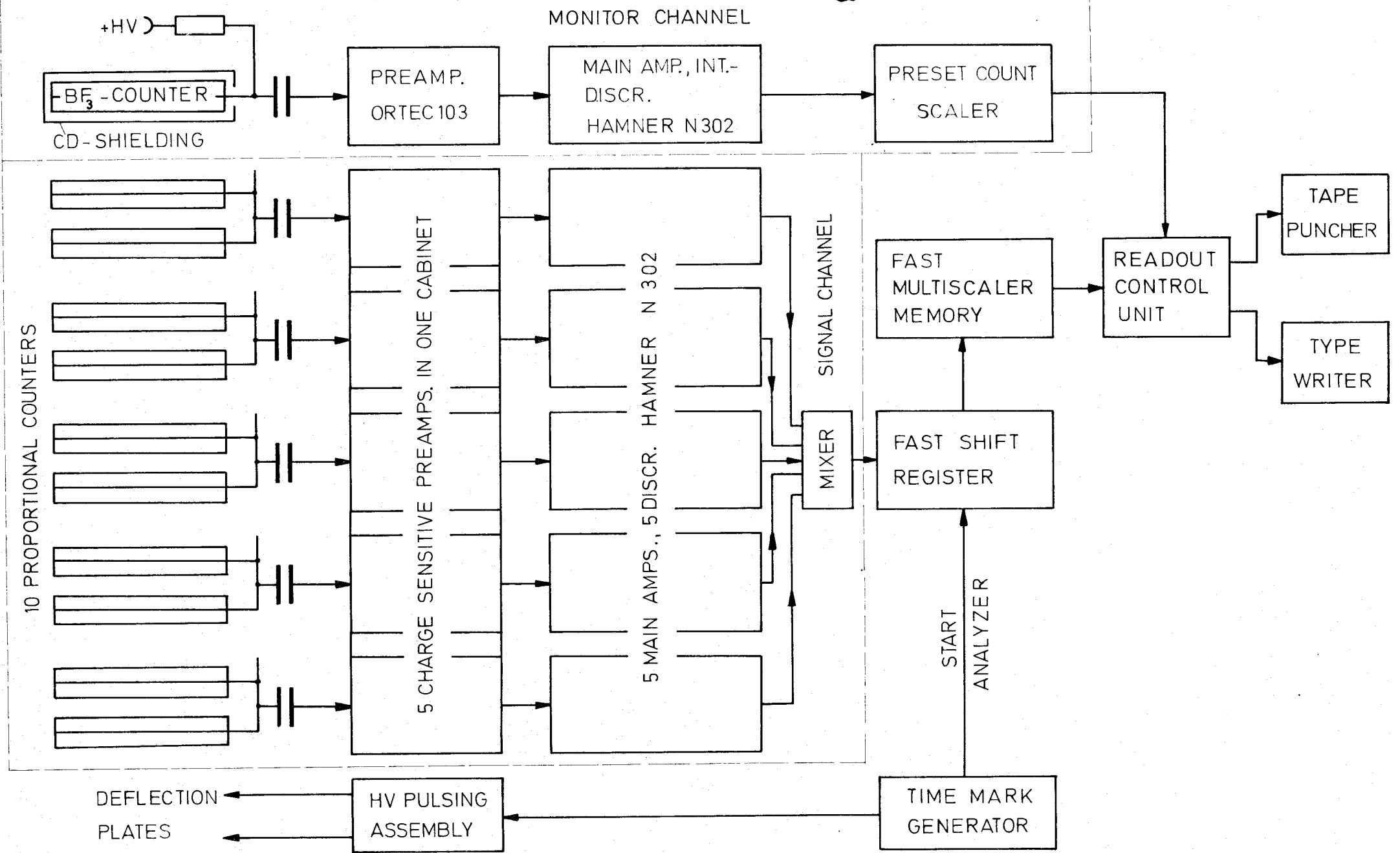


FIG.3 BLOCK DIAGRAMM OF ELECTRONIC CIRCUITRY

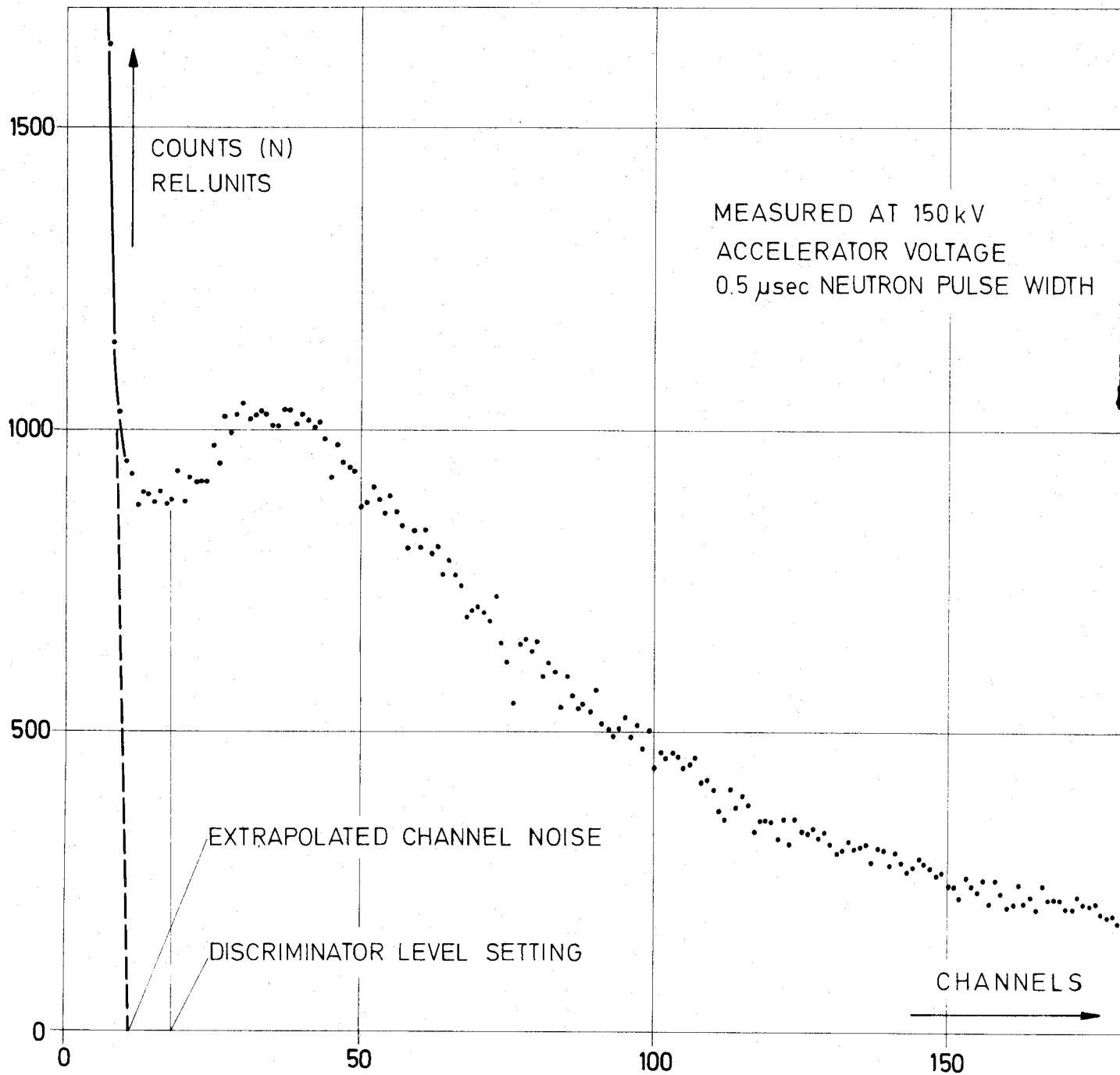


FIG.4  $\gamma$ -SPECTRUM OF A PROPORTIONAL COUNTER



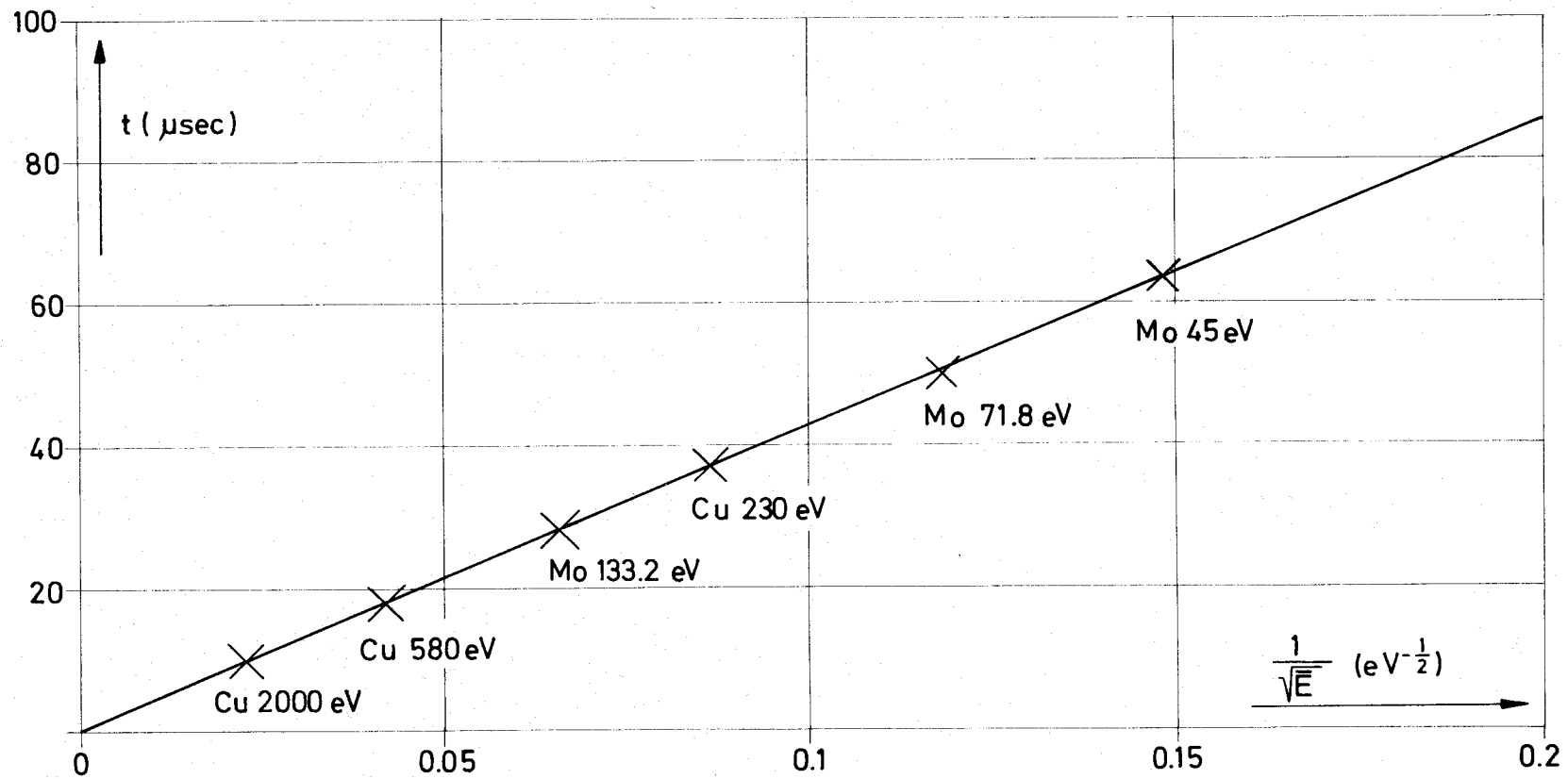


FIG.5 DEPENDENCE OF SLOWING DOWN TIME  $t$  ON  $1/\sqrt{E}$

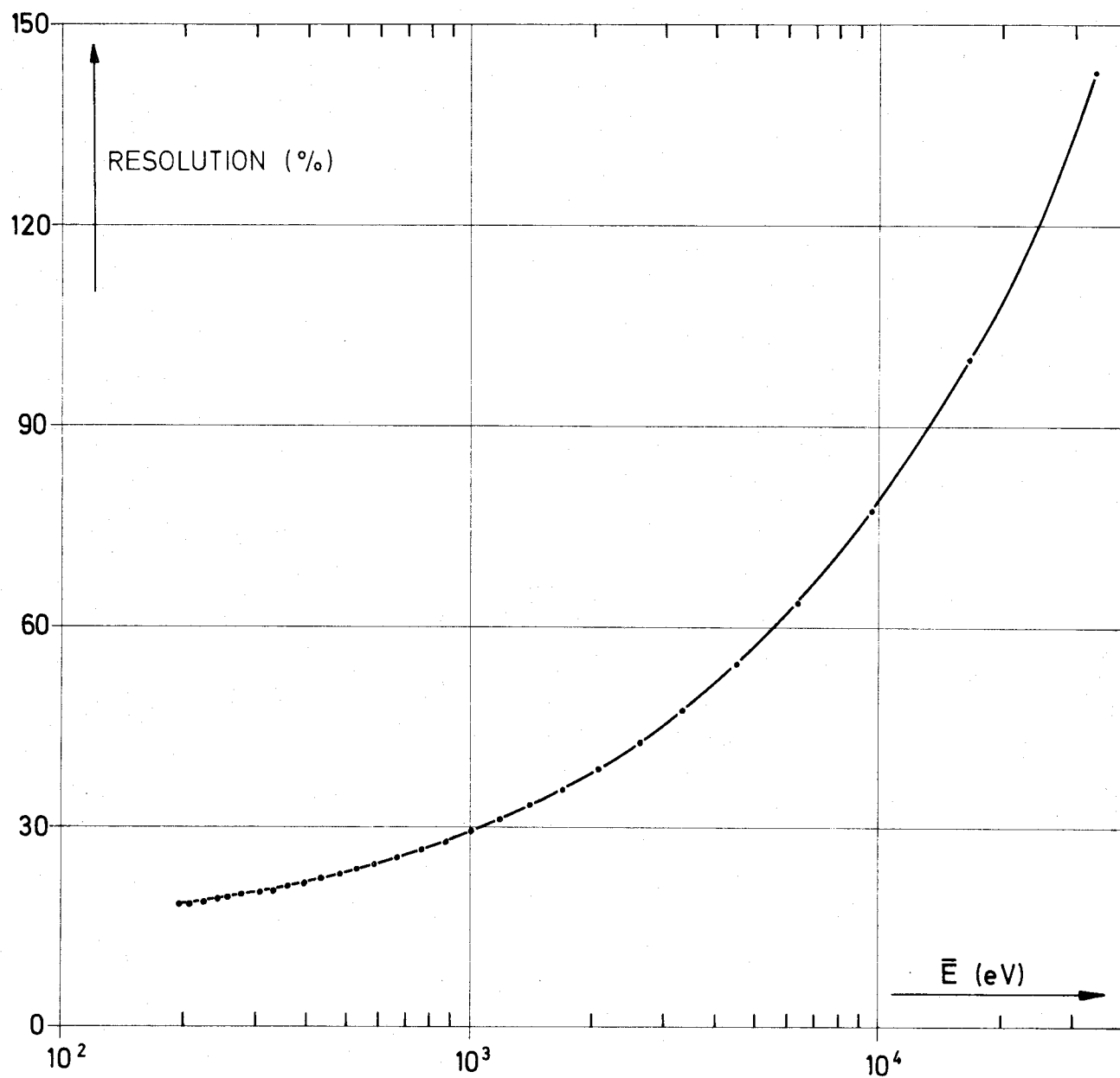


FIG.6 SLOWING DOWN TIME SPECTROMETER RESOLUTION CURVE

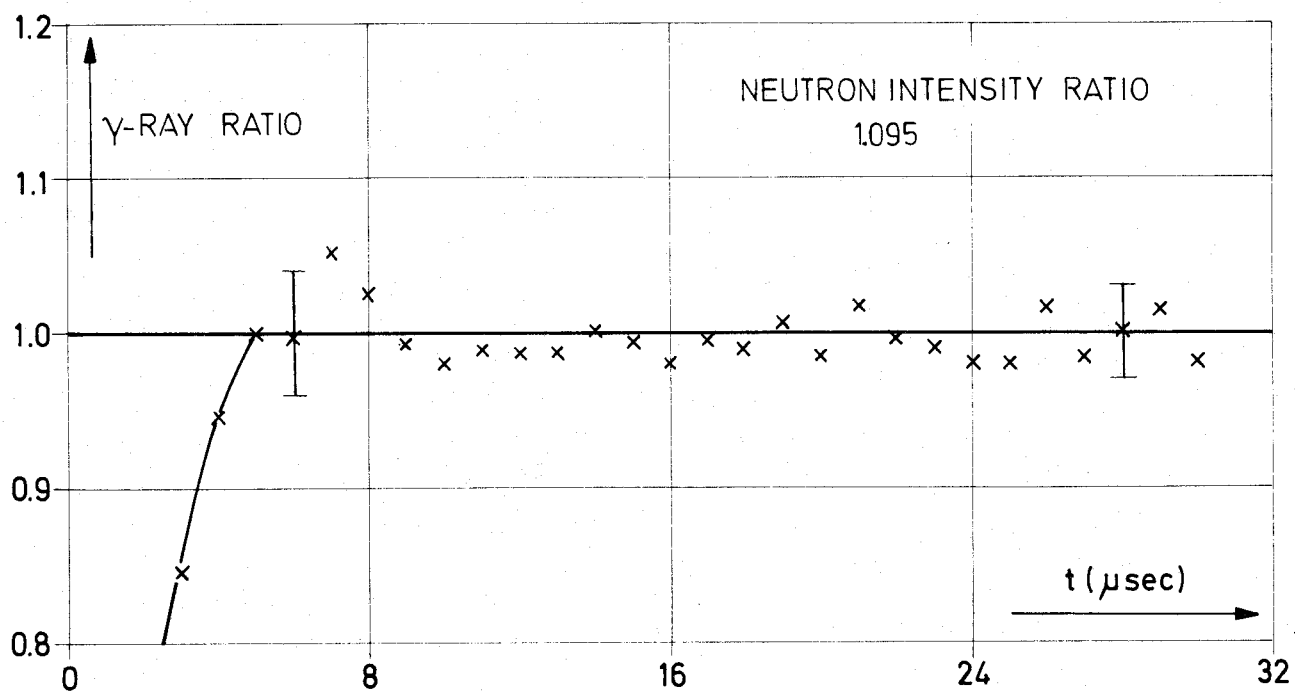


FIG.7 RATIO OF  $\gamma$ -RAYS AT DIFFERENT NEUTRON INTENSITIES

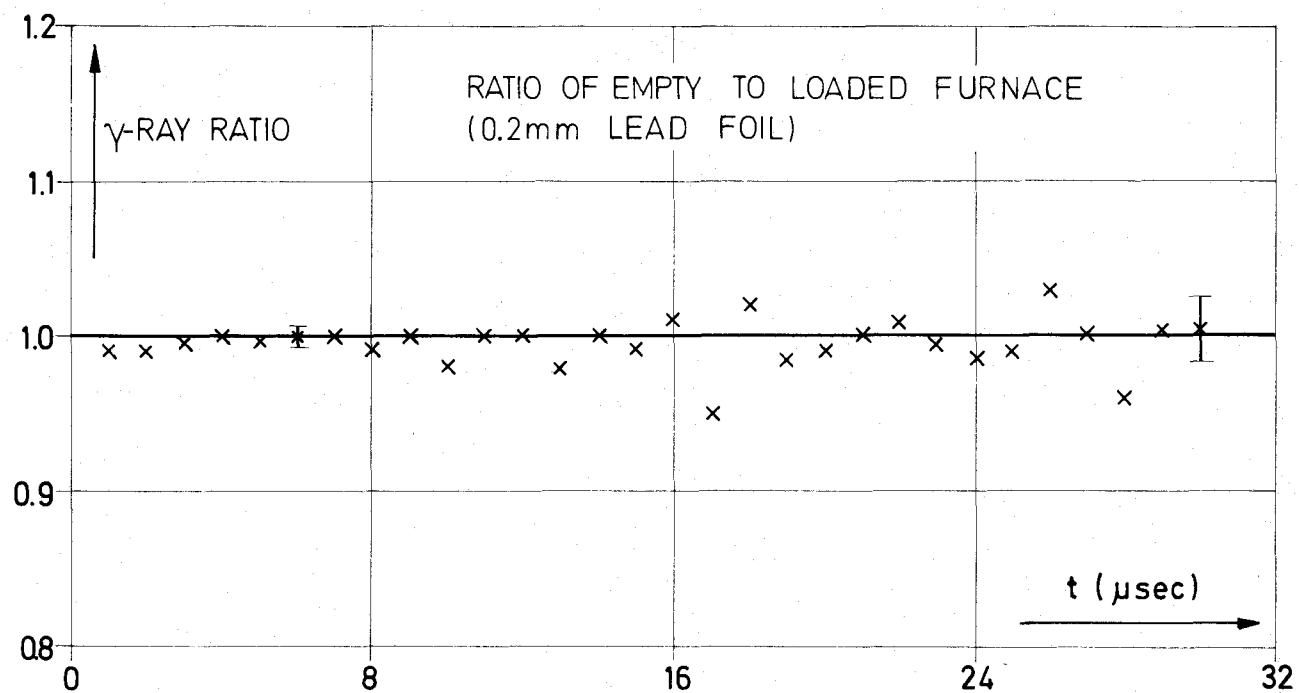


FIG.8  $\gamma$ -RAY RATIO OF A SHIELDING EXPERIMENT

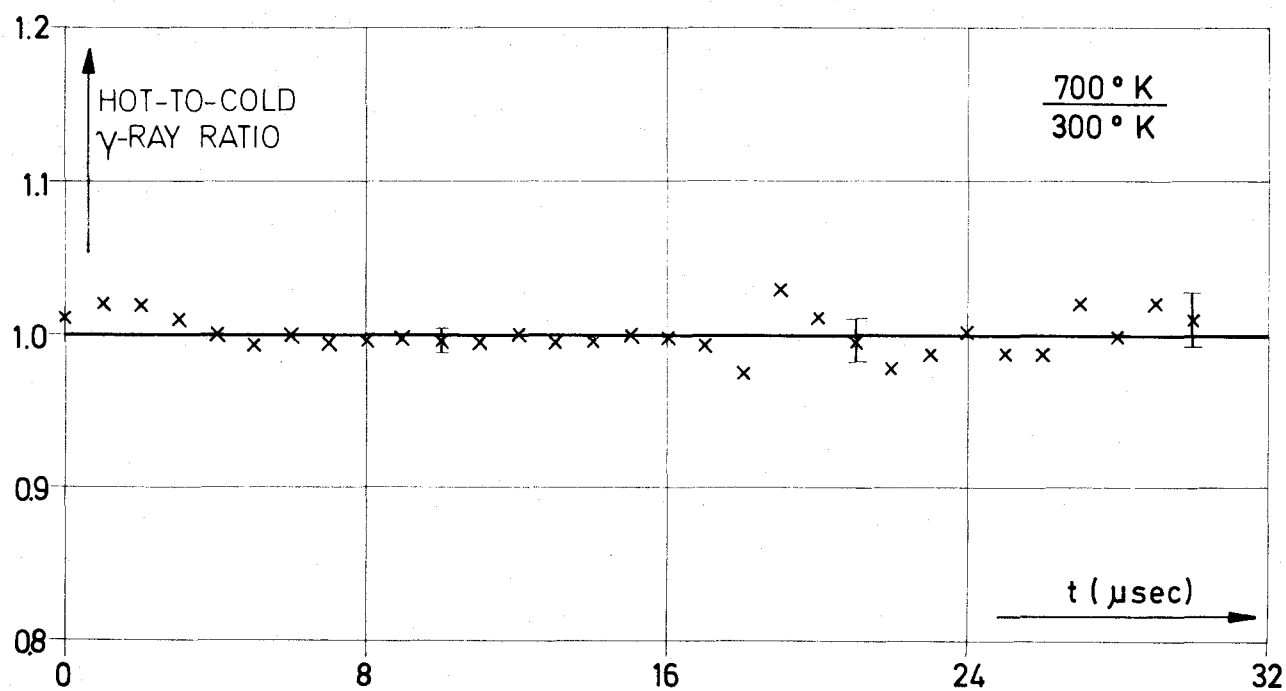


FIG.9 HOT-TO-COLD BACKGROUND  $\gamma$ -RAY RATIO VERSUS SLOWING DOWN TIME

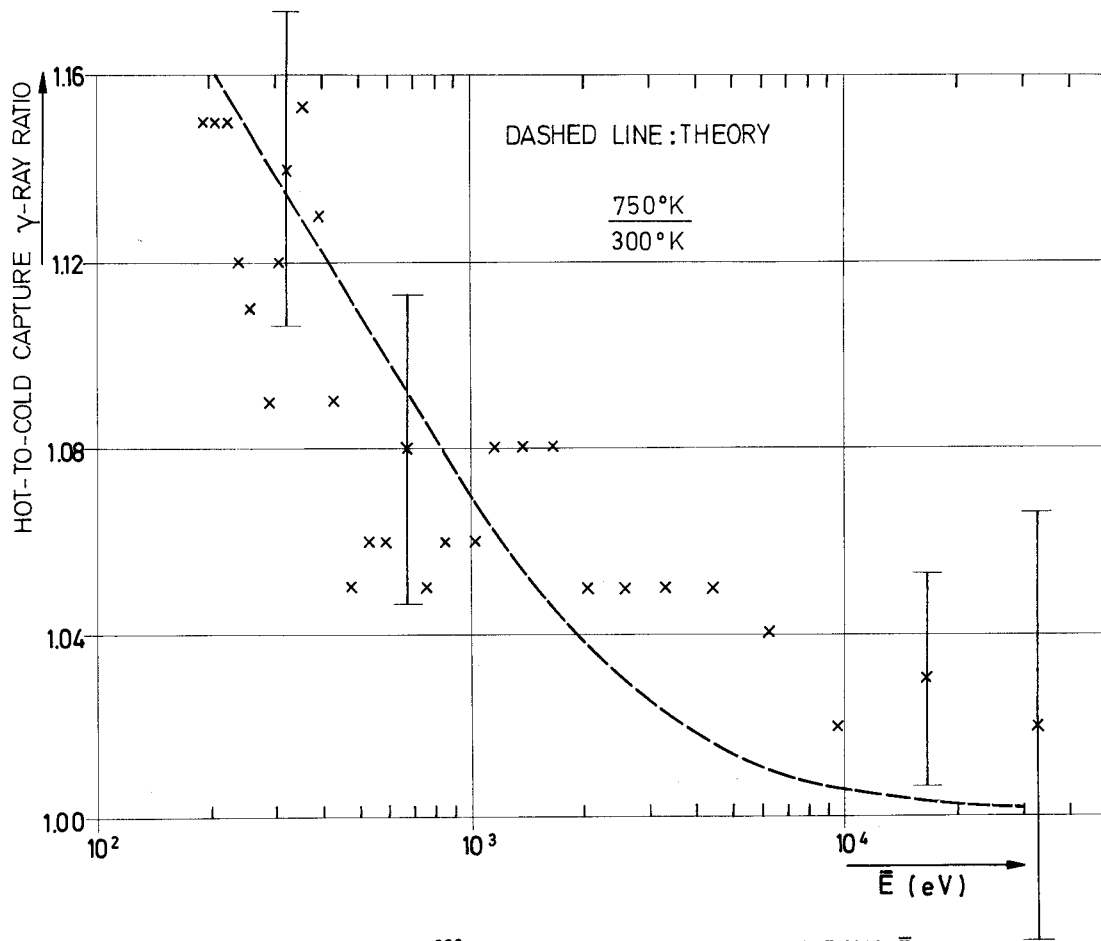


FIG.10 HOT-TO-COLD  $^{238}\text{U}$ -CAPTURE  $\gamma$ -RAY RATIO VERSUS  $\bar{E}$

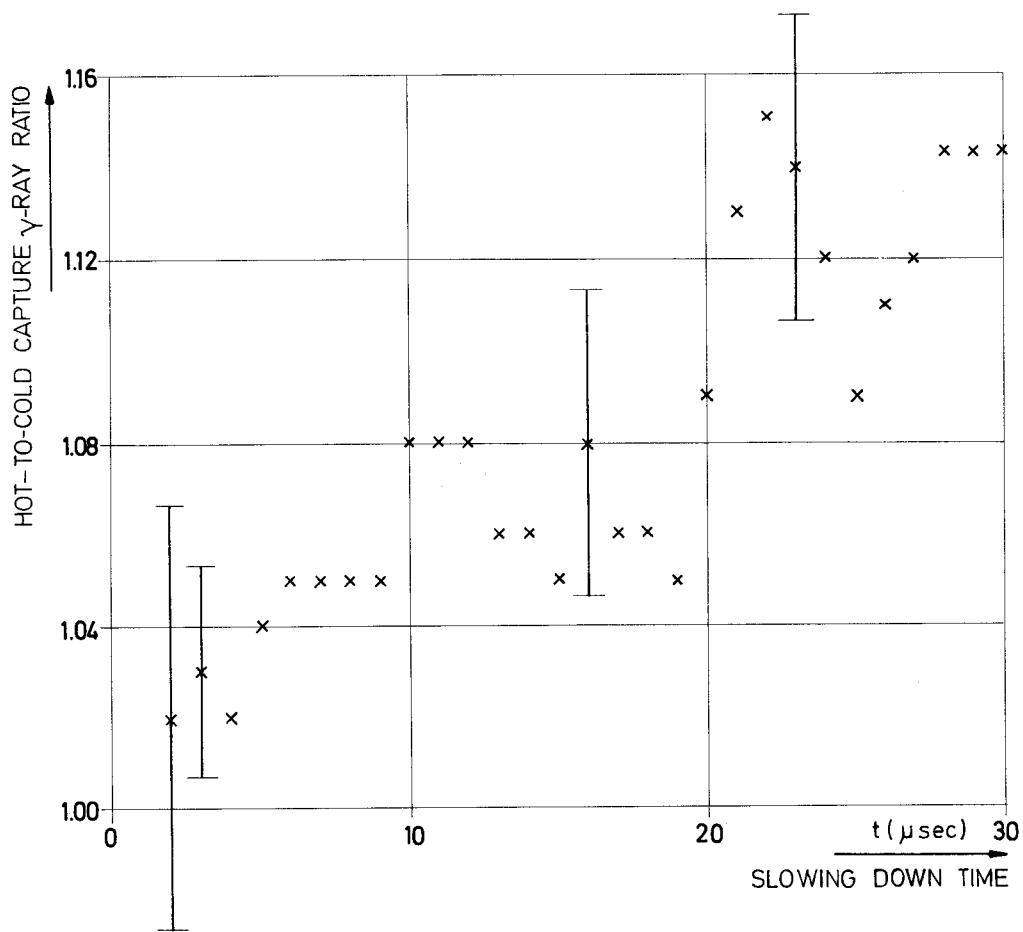


FIG.11 HOT-TO-COLD  $^{238}\text{U}$ -CAPTURE  $\gamma$ -RAY RATIO VERSUS t

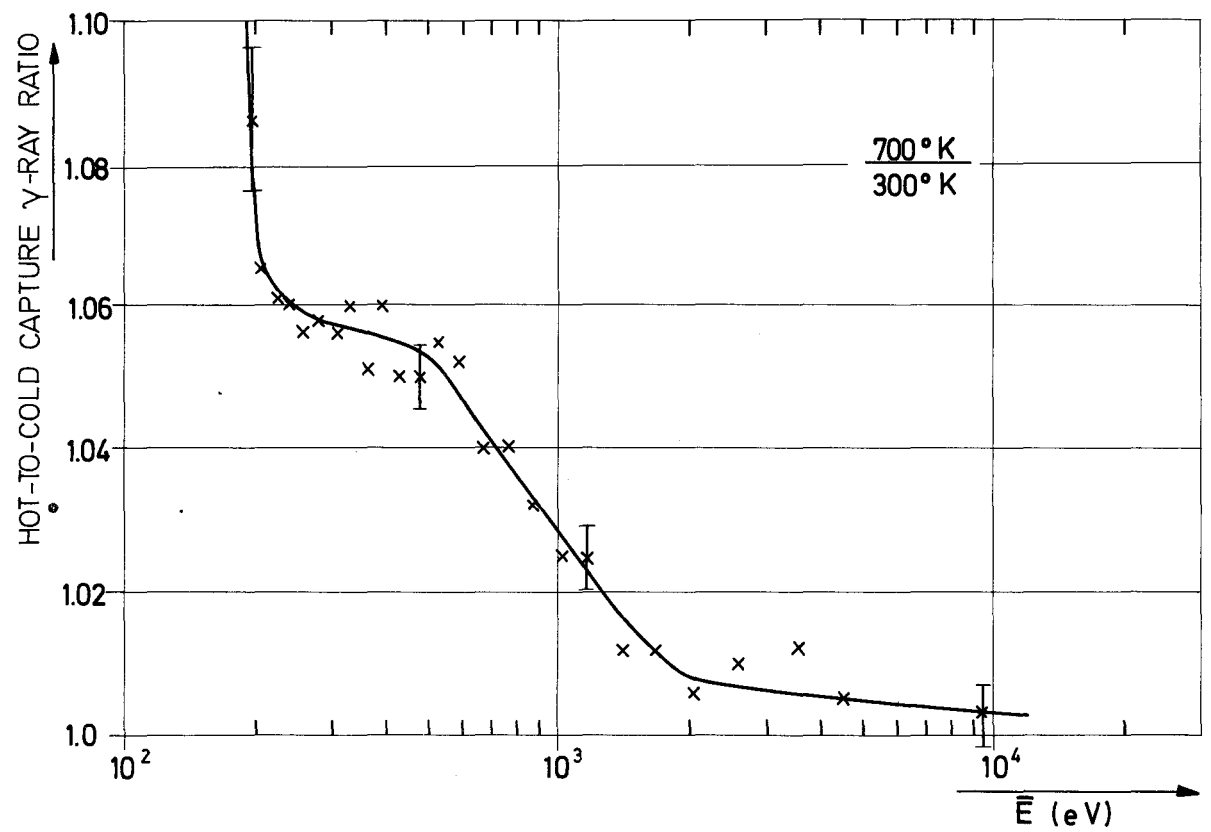


FIG.12 HOT-TO-COLD TANTALUM CAPTURE  $\gamma$ -RAY RATIO VERSUS ENERGY

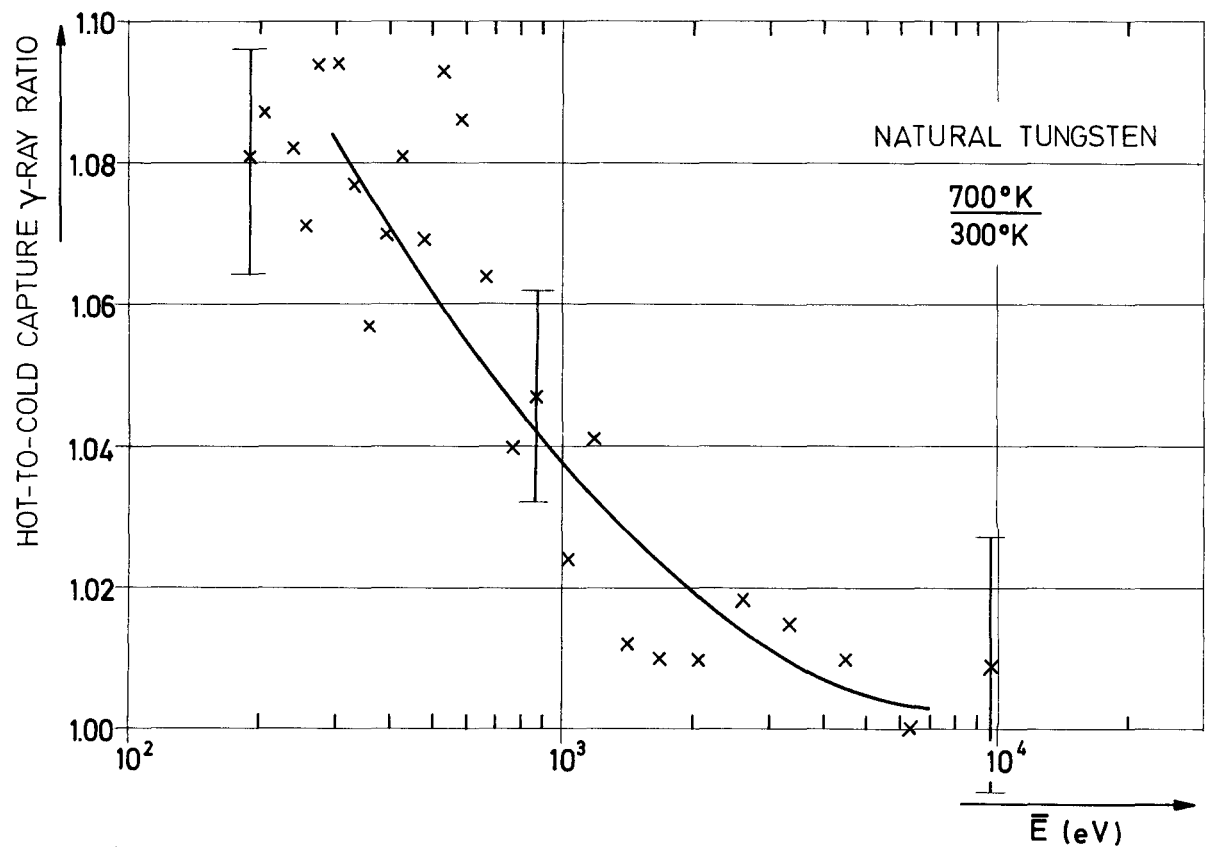


FIG.13 HOT-TO-COLD TUNGSTEN CAPTURE  $\gamma$ -RAY RATIO VERSUS ENERGY



